Non-local couplings, synchronization, pattern formation, and all that

Ricardo Luiz Viana

Departamento de Física, Universidade Federal do Paraná
Curitiba, Paraná, Brasil

Reunião de Trabalho sobre Turbulência em Plasmas
03 de abril de 2014
Instituto de Física da Universidade de São Paulo

Thanks to:

- Fábio Alliguieri dos Santos Silva (UFPR and IFET-Paranaguá-PR)
- Thiago de Lima Prado (UFPR, now in Potsdam-Germany)
- Paulo Paneque Galuzio (UFPR, now in Marseille-France)
- Sérgio Roberto Lopes (UFPR)
- Financial support: CNPq, CAPES, CNEN-RNF (Brazilian Fusion Network)

Introduction

- It is important to characterize the complexity of spatial patterns in many fields of Science and Technology
- Ordered and totally disordered spatial patterns are easier to characterize, but complex patterns pose challenges
- Our work: we use recurrence-based quantities to characterize complex spatial patterns
- Picture: landscape near Mount Roraima (northern tip of Brazil)

Complex spatial patterns and astrophysical plasmas

ultraviolet image (SOHO/ESA/NASA)

- textured appearance = solar plasma is constantly in (turbulent) motion
- as the Sun's magnetic field lines get tangled, they create clusters of strong magnetic activity that push around the Sun's surface plasma
- bright spots correspond to active regions
- solar prominence seen erupting at upper right

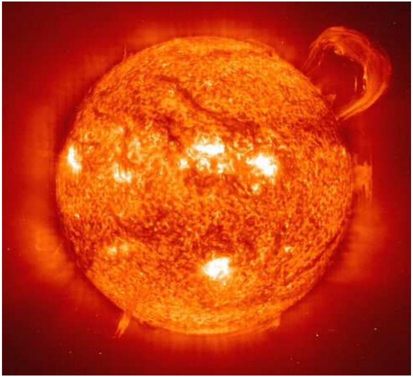

Complex spatial patterns and fusion plasmas

M. W. Jakubowski *et al.*, J. Nucl. Materials **365**, 371 (2007)

- temperature distribution at target plates (TEXTOR tokamak, Jülich, Germany)
- measurements give evaluation of heat flux at tokamak wall
- high temperature regions caused by plasma particles coming from the plasma core (large connection lengths)
- non-uniformity of distribution suggests fractal structures ("magnetic footprints")

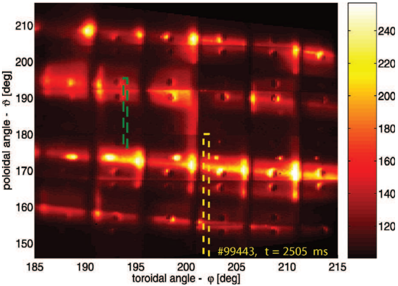

Complex spatial patterns and technological plasmas

S. H. Cho *et al.*, Microelectronic Engn. **77**, 116 (2005)

- AFM image of the surface of polymide (PI) films
- treated by O_2 inductively-coupled plasma
- goal: improvement of the adhesion strength between Cr layer and the PI substrate
- bottom power in the ICP system controls the bombardment energy of oxygen ions in the plasma
- reactive etching of the PI surface leads to the increased morphological surface roughening

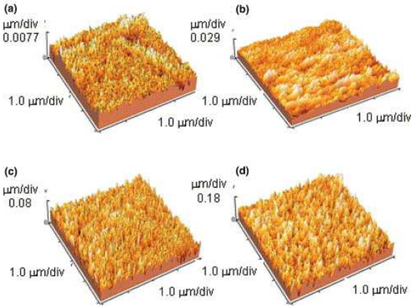

Difficulties in the characterization of complex spatial patterns

- complex profiles are not totally smooth or fractal
- they may contain clusters of spatially ordered interspersed with disordered (rough) region
- they defy usual methods of spatial characterization (RMS roughness or fractal analysis)

One-dimensional spatial patterns

- spatial profile is discretized with steplength Δ: sites at $x_i = i\Delta$
- height at each site $h(i) = h(x = x_i)$
- spatial recurrence: two lattice points i and j have the same value, up to some precision: $|h(i) - h(j)| \approx \ell$
- spatial recurrence matrix elements

$$R_{ij} = \Theta(\ell - |h(i) - h(j)|),$$

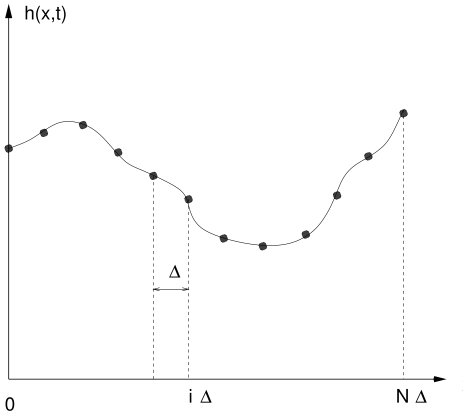

Spatial recurrence plots

- graphical representation of the spatial recurrence matrix
- thresholded: $R_{ij} = 1$ (black pixel) or 0 (white pixel)

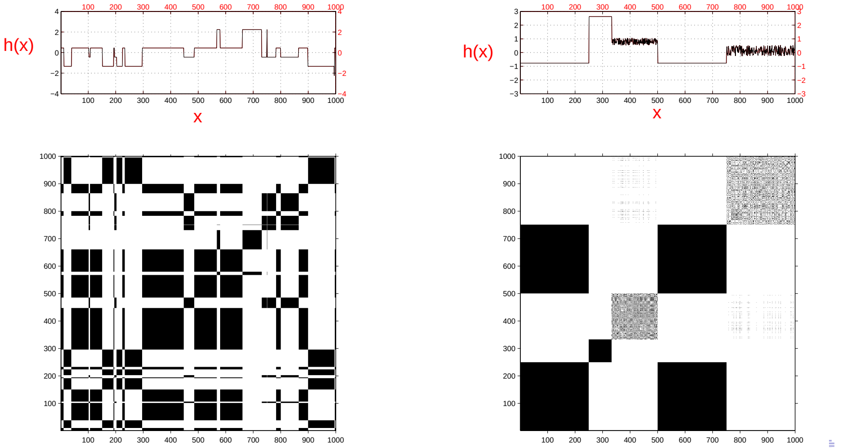

Structures in a spatial recurrence plot and quantification

- Horizontal or vertical structures → smooth plateaus or elevations with small slope
- Diagonal structures → spatially correlated points: sloped lines, curvy segments
- Principal diagonal line always exists by construction of R_{ij}
- Isolated points → parts of the profile with little or no spatial correlation with its neighbors
- white bands → existence of "defects" (irregular clusters)
- recurrence rate: probability of finding spatially recurrent point

$$REC = \frac{1}{N^2} \sum_{i=1}^{N} \sum_{j=1, j \neq i}^{N} R_{ij}.$$

- laminarity: fraction of pixels belonging to horizontal structures in a spatial recurrence plot

Non-locally coupled chaotic maps

- non-local coupling: interaction strength decreases with the lattice distance as a power-law (with exponent α)
- local dynamics: chaotic logistic map $f(x) = 4x(1-x)$, with $x \in [0,1]$
- $x_n^{(i)}$: state variable at time n and spatial position $i = 1, 2, \ldots N$ (one-dimensional chain)
- periodic boundary conditions: $x_n^{(i)} = x_n^{(i \pm N)}$, random initial conditions $x_0^{(i)}$

$$x_{n+1}^{(i)} = (1-\varepsilon) f(x_n^{(i)}) + \frac{\varepsilon}{\eta(\alpha)} \sum_{j=1}^{N'} \frac{[f(x_n^{(i+j)}) + f(x_n^{(i-j)})]}{j^\alpha}$$

- normalization factor: $\eta(\alpha) = 2 \sum_{j=1}^{N'} j^{-\alpha}$

Spatial patterns and spatial recurrence plots

- $N = 1001$ maps with $\varepsilon = 1.0$ and (a) $\alpha = 2.0$, (b) 2.8
- Top: spatial pattern at fixed time $n = 2001$
- Bottom: spatial recurrence plot with cutoff radius $\ell = 0.05$

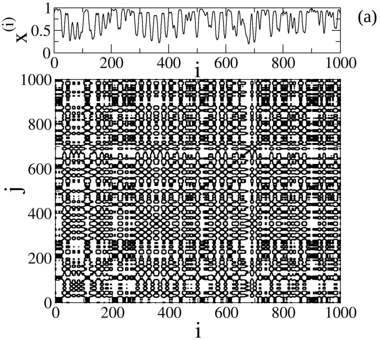

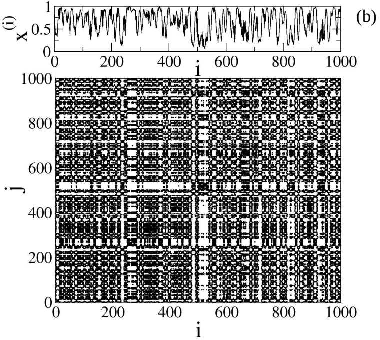

Detecting synchronized patterns using spatial recurrences

- synchronized patterns

$$x_n^{(1)} = \ldots = x_n^{(N)}$$

- large laminarity corresponds to complete synchronization
- transition to non-synchronized behavior as α increases (coupling becomes more local)
- $\alpha \to \infty$: local (nearest-neighbor) coupling
- $\alpha \to 0$: global (all-to-all) coupling

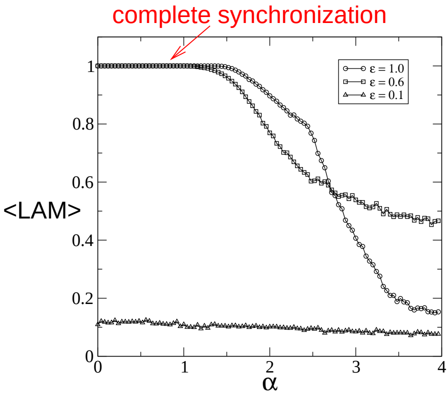

Two-dimensional spatial patterns

- two-dimensional pattern h_{ij} of N sites
- at each site we take a square block of side N' and compute the recurrence rate of h_{ij} with all the other sites belonging to this block
- we obtain a recurrence-rate matrix with elements

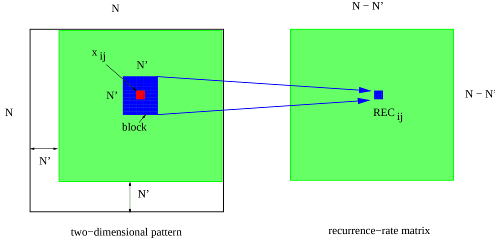

$$REC_{ij} = \frac{1}{N'^2} \sum_{k=i}^{i+N'} \sum_{\ell=i}^{i+N'} \Theta\left(\ell - |h_{ij} - h_{k\ell}|\right),$$

Reaction-diffusion equations

- activator-inhibitor system

$$\frac{\partial u}{\partial t} = f(u, v) + D_u \nabla^2 u$$

$$\frac{\partial v}{\partial t} = g(u, v) + D_v \nabla^2 v$$

- $u(\mathbf{r}, t)$: local concentration of an activator species
- $v(\mathbf{r}, t)$: idem for an inhibitor species
- $f(u, v)$ and $g(u, v)$: local dynamics of the reaction (rate equations)
- local coupling with different diffusion coefficients D_u and D_v
- basic ingredients: mass conservation and Fick's law (diffusion flux proportional to the concentration gradient)

Reaction-diffusion equations in a square lattice

- two-dimensional lattice with spacing Δ
- discretized variables $k, j = 0, 1, \ldots (N-1)$

$$u_{k,j}(t) = u(x = k\Delta, y = j\Delta, t),$$

$$v_{k,j}(t) = v(x = k\Delta, y = j\Delta, t),$$

- discretized system of ODE's

$$\frac{du_{k,j}}{dt} = f(u_{k,j}, v_{k,j}) + \frac{D_u}{4}\left(u_{k+1,j} + u_{k-1,j} + u_{k,j+1} + u_{k,j-1} - 4u_{k,j}\right)$$

$$\frac{dv_{k,j}}{dt} = g(u_{k,j}, v_{k,j}) + \frac{D_v}{4}\left(v_{k+1,j} + v_{k-1,j} + v_{i,k+1} + v_{i,k-1} - 4v_{k,j}\right)$$

Reaction-diffusion equations with nonlocal coupling

- diffusion flux does not depend only on the local gradients but on a wider vicinity of each point
- yields a (non-linear) integro-differential equation

$$\frac{\partial u}{\partial t} = f(u, v) + D_u \int d^2\mathbf{r}' \sigma(\mathbf{r}, \mathbf{r}') u(\mathbf{r}', t),$$

$$\frac{\partial v}{\partial t} = g(u, v) + D_v \int d^2\mathbf{r}' \sigma(\mathbf{r}, \mathbf{r}') v(\mathbf{r}', t)$$

- $\sigma(\mathbf{r}, \mathbf{r}')$ is a non-local interaction kernel
- if the coupling is mediated by a third (locally) diffusing substance then $\sigma(r) \sim K_0(r)$ in the fast relaxation limit (Kuramoto and Nakao)
- another example is a power-law kernel: $\sigma(r) \sim r^{-\alpha}$

Reaction-diffusion equations in a square lattice with powerlaw coupling

$$\frac{du_{k,j}}{dt} = f(u_{k,j}, v_{k,j}) - D_u u_{k,j} + \frac{D_u}{\kappa(\alpha)} \sum_{r=-N'}^{N'}{}^{\star} \sum_{\ell=-N'}^{N'}{}^{\star} \frac{u_{k+r,j+\ell}}{(r^2+\ell^2)^{\alpha/2}}$$

$$\frac{dv_{k,j}}{dt} = g(u_{k,j}, v_{k,j}) - D_v v_{k,j} + \frac{D_v}{\kappa(\alpha)} \sum_{r=-N'}^{N'}{}^{\star} \sum_{\ell=-N'}^{N'}{}^{\star} \frac{v_{k+r,j+\ell}}{(r^2+\ell^2)^{\alpha/2}}$$

- $N' = (N-1)/2$, with N odd,
- starred sums: we exclude from them the terms with $r = \ell = 0$
- normalization factor

$$\kappa(\alpha) = \sum_{r=-N'}^{N'}{}^{\star} \sum_{\ell=-N'}^{N'}{}^{\star} \frac{1}{(r^2+s^2)^{\alpha/2}}$$

Local dynamics of activator-inhibitor system

- Meinhardt and Gierer model [RMP **66**, 1481 (1994)]

$$f(u,v) = 0.01\left(\frac{u^2}{v} - u\right) \qquad g(u,v) = 0.02\left(u^2 - v\right)$$

- activator undergoes an auto-catalytic reaction with inhibition and degradation
- inhibitor also increases with activator and suffers degradation
- two equilibria: $(0,0)$ (unstable) and $(1,1)$ (asymptotically stable)
- these are also equilibria for the **coupled** system
- Turing instability: a formerly stable spatially homogeneous pattern becomes inhomogeneous as the diffusion coefficients are changed
- pattern formation occurs after linearly unstable modes suffer saturation (due to the nonlinearity of the local dynamics)

Spatial patterns in the locally coupled case ($\alpha = 1000$)

- 101×101 cells, $D_u = 0.016$, $D_v = 0.2$, activator concentration in colorscale
- Left: spatial pattern (fixed time): "zebra" patterns (fingering - lateral inhibition)
- Right: recurrence-rate matrix (blocks of size $N' = 20$): $REC \sim 0.25 - 0.29$, not spatially homogeneous

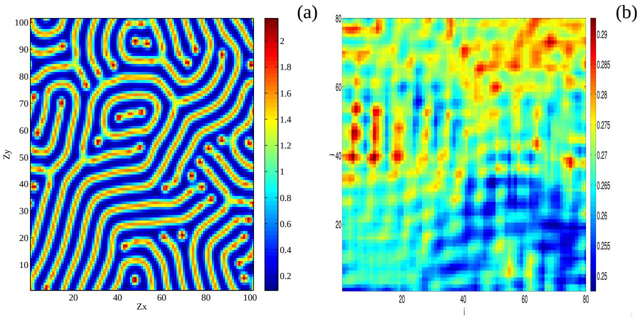

Spatial patterns in the locally coupled case ($\alpha = 1000$)

- 101×101 cells, $D_u = 0.005$, $D_v = 0.2$
- Left: spatial pattern (fixed time): spot "leopard" patterns (fingering - lateral inhibition)
- Right: recurrence-rate matrix: $REC \sim 0.74 - 0.81$, locally recurrent regions

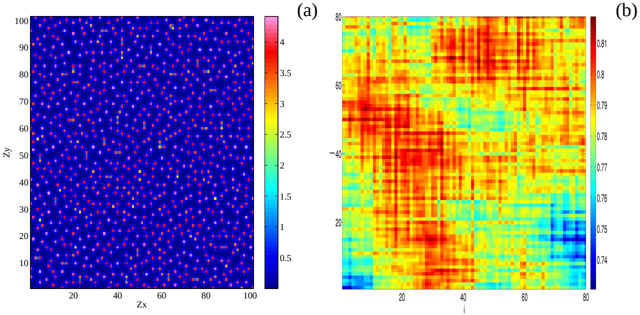

Spatial patterns in the intermediate coupled case ($\alpha = 1$)

- 101×101 cells, $D_u = 0.015$, $D_v = 0.2$
- Left: spatial pattern (fixed time): regular (sinusoidal) pattern
- Right: recurrence-rate matrix: $REC \sim 0.3 - 0.9$, lower-concentration background more recurrent than crests

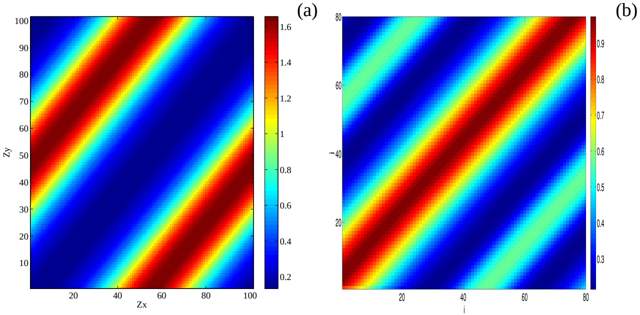

Spatial patterns in the intermediate coupled case ($\alpha = 1$)

- 101×101 cells, $D_u = 0.005$, $D_v = 0.2$
- Left: spatial pattern (fixed time): spots again but with higher concentration (squeezing effect)
- Right: recurrence-rate matrix: capable to detect very subtle differences in spatial patterns due to localized structures

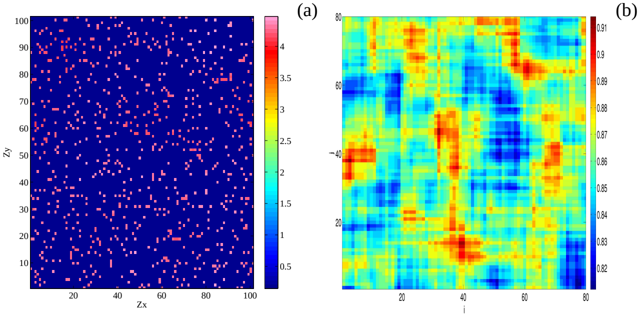

Spatial patterns produced by mammographic images

- scanned mammographic images (LAPIMO, USP, S. Carlos)
- transformed into integer grey-level matrices $\rightarrow$ lossless image files with $65,000$ levels
- very sensitive to differences in grey-levels $\rightarrow$ detection of structures barely visible to the naked eye (tumours)

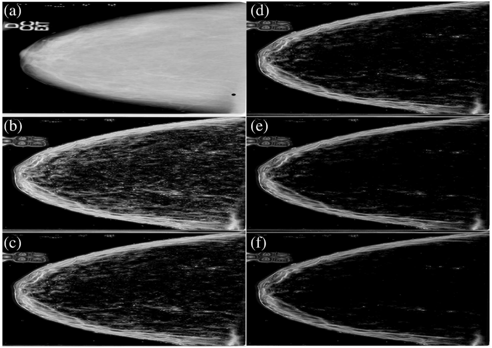

Conclusions

- complex spatial patterns have coexistent ordered and disordered parts
- we developed recurrence-based numerical diagnostics for characterization of complexity in spatial patterns (1D and 2D)
- they are good indicators of synchronized states
- spatio-temporal dynamical systems: patterns in reaction-diffusion equations (activator-inhibitor)
- recurrence-based diagnostics are very sensitive to pattern changes
- analysis of images: structures in digital mammographic images

Thank you very much.

Publications

- D. B. Vasconcelos, S. R. Lopes, R. L. Viana, and J. Kurths: Phys. Rev. E **73**, 56207 (2006)
- F. A. S. Silva, R. L. Viana, T. L. Prado, and S. R. Lopes, Comm. Nonlin. Sci. Numer. Simulat. **19**, 1055 (2014)
- T. L. Prado, P. P. Galuzio, S. R. Lopes, and R. L. Viana, Chaos **24**, 013106 (2014)
- F. A. S. Silva, R. L. Viana, and S. R. Lopes, *Pattern formation and Turing instability in an activator-inhibitor system with power-law coupling*, preprint (2014)

available for download at: http://fisica.ufpr.br/viana